

Transient nucleation with a monotonically changing barrier

Vitaly A. Shneidman

Department of Physics, New Jersey Institute of Technology, Newark, New Jersey 07102, USA

(Received 22 June 2010; published 10 September 2010)

Nucleation is considered for nonzero rate of change of the dimensionless barrier B , which is characterized by a finite, slowly varying “nonstationary index” $\mathcal{N} \propto -(dB/dt)$. In the standard adiabatic approximation it is assumed that after the start of nucleation an \mathcal{N} -independent nucleation flux is established instantaneously, with a quasi-steady-state (QSS) value determined by the current barrier $B(t)$. Those assumptions, however, can be justified only in the strict limit $\mathcal{N} \rightarrow 0$, and otherwise both transient nucleation at small times, and subsequent deviations from QSS are essential. Earlier results for the non-QSS transient flux are refined and generalized to account for arbitrary relations between the rates of the change of the barrier and of the critical size, and for a variable $\mathcal{N}(t)$. The \mathcal{N} -dependent transient distributions of growing nuclei and their numbers also are obtained. The treatment is mostly based on matched asymptotic (singular perturbation) analysis of the Becker-Döring equation (BDE), and involves comparison with exact numerics. General results are specified within the continuous Zeldovich-Frenkel approximation to BDE, with a large fixed critical size and a barrier which either increases ($\mathcal{N} < 0$) or decays ($\mathcal{N} > 0$) with time. In such cases growth can be described exactly, allowing to extend the nucleation solution to arbitrary sizes without additional approximations. Resulting distributions $f(r, t)$ are monotonic in size r for $\mathcal{N} \geq 0$, with a diverging total number of particles ρ as $t \rightarrow \infty$. For $\mathcal{N} < 0$ distributions acquire an asymmetric bell shape with a finite ρ , which is exponentially small compared to ρ^{QSS} .

DOI: [10.1103/PhysRevE.82.031603](https://doi.org/10.1103/PhysRevE.82.031603)

PACS number(s): 64.60.Q–

I. INTRODUCTION

Fluctuational formation of particles of a new phase, or *nucleation* is an essentially time-dependent phenomenon due to a finite lifetime of a metastable state. The main control parameter is the dimensionless nucleation barrier B , and in a typical experimental study B first has to be reduced from near-infinite values near phase equilibrium to values of several tens in order to make nucleation observable. Classical examples include a rapid pressure drop, which initiates cavitation in a fluid [1], rapid expansion of a condensing vapor [2] (see also recent [3,4]), etc. Quenching of glass-forming melts [5–7] or pulse-laser melted thin silicon films [8,9] also could be mentioned. During later stages of nucleation, B is increased, either due to external control (e.g., heating in crystallization problems [10,11]), or due to exhaustion of the metastable phase and release of latent heat by growing nuclei [9]. Of special status are transient nucleation crystallization experiments [12] with an extended intermediate stage when the barrier is held fixed.

Traditional approaches to describe nucleation under time-dependent conditions are based on the so-called adiabatic or “quasi-steady-state” (QSS) approximation. In this approximation the nucleation rate is associated with the stationary flux j_s of the nucleation equation written in the space of sizes R of the nuclei, with coefficients “frozen” at the current instant of time. There are many attractive features in the QSS description due to insensitivity of j_s either to the rate of the barrier change, or to the size R where the flux is evaluated. Associated growth is also simplified, leading to a straightforward scaling of the distribution of nuclei over sizes or of their total number as functions of quench [7] or heating rates [13] in glass crystallization problems. Generalizations of the QSS approach to include depletion by growing nuclei [14] and for heterogeneous nucleation [15] are available. Yet, in

many situations justification of the QSS approximation is insufficient, and one expects either transient effects, or those due to time-dependence of the barrier, to be important. An alternative to QSS description would be direct numerical solution of various versions of the Becker-Döring equation (BDE) which are discussed, e.g. in condensation [2,4] or crystallization [6,10,16,17] applications. In many cases, however, a large number of required input parameters blurs the universal aspects of the observed dependences, which are often determined by only a few dominant scaling variables, and in this sense the analytical study attempted in the present paper can be helpful. At the same time, within a selected input numerics has an unsurpassed level of accuracy, and can be used to assess the reliability of analytical conclusions.

The major goal of this study is thus to derive and test numerically a non-QSS expression for the distribution of nuclei, which would be valid for both signs of dB/dt , and which would include transient effects. Associated fluxes and numbers of nuclei, which can have direct experimental relevance, also will be considered. The method will be based on generalization of the matched asymptotic solution (MAS) of the BDE, earlier discusses in the context of cavitation [18,19], vapor condensation [20(a)] and crystallization [7,20(b),20(c)]. A mathematically similar situation of nucleation of particles with finite lifetimes also can be mentioned [21]. From a technical point, the MAS is straightforward in case the barrier and other parameters are fixed (or piecewise constant) in time, and the distribution evolves toward the steady-state [20,22]. In such situations, known as “transient” (or “nucleation pulse”) problems, accuracy of MAS is determined solely by large values of B , while growth can be described exactly, allowing to extend the solution to arbitrary sizes R . For a general time dependence, however, additional restrictions on the rate of change of coefficients and approximations for growth are generally required, which explains detailed comparison with exact numerics in the present work.

On a qualitative level, an important remaining question is whether the non-QSS effects are primarily due to the rapid change of the barrier $B(t)$ or to that of the critical size $R_*(t)$? A definite conclusion was hard to reach here based on past studies, which usually considered B and R_* closely linked to each other. To clarify the issue, a more general situation with arbitrary, though time-independent value of $\nu = d \ln R_*/d \ln B$ will be considered. Furthermore, results will be specified for $\nu=0$, when only the barrier changes with time, and it will be shown that even in this extreme the non-QSS effects can be quite strong.

II. BACKGROUND

A. Nucleation equation and steady-state solution

According to Ref. [1] (see also a textbook description in Ref. [23]) nucleation can be viewed as a random walk of nuclei in the R -space, and is described by a Fokker-Plank type equation

$$\frac{\partial f}{\partial t} = -\frac{\partial j}{\partial R}, \quad j = -\beta \frac{\partial f}{\partial R} + \dot{R}f \quad (1)$$

with diffusivity $\beta(R) > 0$ and with \dot{R} being the deterministic growth rate which changes sign at the critical size R_* . A discrete version of Eq. (1) written in the n -space, the number of monomers in a nucleus, is known as the ‘‘Becker-Döring equation’’ (BDE) and is presented in Sec. IV.

The flux j is identically zero for a (quasi)equilibrium distribution

$$f^{eq}(R) = A(R) \exp(-W/kT) \quad (2)$$

with $W(R)$ being the minimal work required to form a nucleus, usually taken in the form

$$\frac{1}{kT} W = B\phi(r), \quad \phi(r) = 3r^2 - 2r^3 \quad (3)$$

with $r \equiv R/R_*$, and B being the dimensionless barrier. The pre-exponential $A(R)$ cannot be defined within the macroscopic classical approach [23] but is assumed to be a smooth, power-law type function, traditionally taken as $A \propto R^2$, corresponding to a constant in the n -space. Neglecting the derivative of the pre-exponential compared to that of a large barrier, one can write an ‘‘Einstein relation’’ in the R -space [1], connecting β to the growth rate,

$$\dot{R} = -\frac{\beta}{kT} \frac{\partial W}{\partial R} = -\beta \frac{B}{R_*} \phi'(r). \quad (4)$$

Boundary conditions are taken as

$$f/f^{eq} \approx 1, \quad R \ll R_* \quad \text{and} \quad f/f^{eq} \rightarrow 0, \quad R \gg R_*. \quad (5)$$

Introducing the time scale

$$\tau = \left(\frac{d\dot{R}}{dR} \bigg|_{r=1} \right)^{-1} \quad (6)$$

the asymptotic steady-state solution to Eq. (1) for $B \gg 1$ can be written as

$$j_s = \frac{\Delta}{2\tau\sqrt{\pi}} f^{eq}(R_*), \quad \Delta = \left\{ -\frac{B}{2} \phi''(1) \right\}^{-1/2} R_*. \quad (7)$$

The above expression, which can be traced to the work of Zeldovich [1], is accurate not only for the continuous Eq. (1), but also for the discrete BDE, as long as the critical nucleus contains at least a handful of monomers n_* [24]. Equation (7) is also remarkably insensitive to physical mechanism of mass exchange between the nucleus and the metastable phase, once the time scale τ has been determined. Otherwise, the type of mass exchange affects the deterministic growth. Within the continuous description, the standard selections are

$$\dot{R} = \frac{R_*}{\tau} r^{-\theta} \left(1 - \frac{1}{r} \right). \quad (8)$$

Here $\theta = -1$ corresponds to cavitation [1] with no mass exchange, while $\theta = 1$ and 0 correspond to diffusion- and interface-limited mechanisms, respectively. The counterpart of the latter case for the Turnbull-Fisher version of the discrete BDE (see Sec. IV below) is given by $\dot{R} = (2R_*/a\tau) \sinh[\frac{a}{2}(1-1/r)]$ [6]. For small $a = 2B/n_*$ the discreteness corrections are minor [25].

The steady-state distribution of growing nuclei is given by

$$f_s(R) = j_s/\dot{R}, \quad R - R_* \gg \Delta \quad (9)$$

It is characterized by a power-law tail R^θ as $R \rightarrow \infty$, and is singular near the critical size.

The QSS description of nucleation assumes that the rate is still given by Eq. (7), but with time-dependent values of parameters. The QSS growth corresponds to the large- R asymptote of Eq. (8)

$$\dot{R}^{QSS} = \frac{R_*}{\tau} r^{-\theta}. \quad (10)$$

Except for the special case $\theta = -1$, an attempt to keep the term $1-1/r$ in the growth rate with otherwise QSS description of the flux would prevent smooth matching of nucleation and growth regions, making the results sensitive to selection of the initial size from which growth starts. The distribution is then given by

$$f^{QSS}(R, t) = j_s(t_r^{QSS})/\dot{R}^{QSS}(t_r^{QSS}), \quad t_r^{QSS} > 0. \quad (11)$$

Here $t_r^{QSS}(R)$ is the ‘‘retarded time’’ corresponding to the instance when a particle nucleated with zero initial size (for $\theta > -1$) will grow to size R by the time t . Once the time dependences $\tau(t)$ and $R_*(t)$ are known, the retarded time can be found analytically since Eq. (10) allows a separation of variables. The QSS distribution abruptly turns zero at $R \geq R^{\max}(t)$ with $t_r^{QSS}(R^{\max}) = 0$; this corresponds to an instantaneous ‘‘switch-on’’ of nucleation at $t=0$. If one uses the time units \tilde{t} in which $\tau \equiv 1$, and considers a near-linearly changing barrier $B \approx B_0 - \mathcal{N}\tilde{t}$ and $R_* \approx \text{const}$, as in most examples described below, one has a combination of power-law and exponential factors, with a cutoff at $r^{\max} = [\tilde{t}(\theta+1)]^{1/\theta+1}$,

$$f^{QSS}(r, \tilde{t}) \sim r^\theta \exp\left(-\mathcal{N} \frac{r^{\theta+1}}{\theta+1}\right) \Theta(r^{\max} - r). \quad (12)$$

B. Parameters and notations for time-dependent treatment

Let us switch to dimensionless time

$$\tilde{t} = \int_0^t \frac{dt'}{\tau(t')}, \quad (13)$$

which makes the dimensionless growth rate $dr/d\tilde{t}$ nearly time-independent if R_* changes slowly. The flux is then transformed in accord with

$$j(r,t) \rightarrow \tilde{j}(r,\tilde{t}) = \tau j(r,t) \quad (14)$$

and, similarly, $\tilde{j}_s = \tau j_s$. In order to simplify notation, the *tilde* sign will be dropped in the technical part of the following discussion, although original “physical” units will be restored in figures and when comparing with numerics.

Next, with the new time, let us define a dimensionless “nonstationary index”

$$\mathcal{N} = -dB/dt, \quad (15)$$

which will be the key control parameter, responsible for deviation from QSS. The derivative of the work $W(R)$ is then expressed as

$$-\frac{\partial W}{\partial t kT} = \mathcal{N}(\phi - r\phi'v) \equiv \mathcal{N}\psi(r) \quad (16)$$

and depends on $\nu \equiv d \ln R_*/d \ln B$, the relative rate of change of the critical size compared to that of the barrier. Two extremes can be kept in mind. If the external control parameter is supersaturation (or its analog, pressure, magnetic field, etc.), which determines the inverse of the critical radius, the Gibbs relation $B = 4\pi\sigma R_*^2/3kT$ can be used to obtain $\nu \approx 1/2$ [18,20(a)]. If, on the other hand, supersaturation is fixed and only the temperature is changing, while interfacial tension σ is constant leading to fixed W_* and R_* (as in the Ising model at $T \rightarrow 0$ [26]), one has $\nu \approx 0$. This option will be explored in more detail when comparing with numerics; until then a general, though time-independent $\psi(r)$ is assumed, with $\psi(1) = 1$.

The small parameter for asymptotic treatment is

$$\epsilon \equiv \frac{\Delta}{R_*} = (3B)^{-1/2} \quad (17)$$

and the values of other parameters which appear in the course of the treatment (such as the index \mathcal{N} , the Laplace index p , etc.) are assumed to be ϵ -independent, although they can be large or small compared to 1.

C. Transient nucleation for $\mathcal{N}=0$

A combination of matched asymptotic and Laplace transformation techniques [20](a) gives the following transient flux

$$j(r,t) = j_s \exp[-\exp(-t_r)], \quad t_r = t - t_i(r) \quad (18)$$

with the “incubation time” t_i related to the deterministic growth rate $\dot{r}(r)$ by [20](b)

$$t_i(r) = \mathbf{P} \int_0^r \frac{dr}{\dot{r}} + \ln(6B) - 2C', \quad C' = \int_0^1 dr \left(\frac{1}{\dot{r}} - \frac{1}{r-1} \right) \quad (19)$$

Here \mathbf{P} indicates the principal value of the integral, and for integer θ in the growth rate (8) this integral can be evaluated in elementary functions [20](b) - see Sec. IV below. Other relevant results, such as the total number of nuclei, will be reproduced as the small- \mathcal{N} limit of the more general expressions derived below.

III. RESULTS

A. Approximation of the Laplace transform

The treatment closely follows that of Refs. [19,20(a)], although using a different time variable defined in Eq. (13), and contains a generalization for an arbitrary function ψ in Eq. (16). Also, the earlier inversion technique based on summation over residues will be augmented by the convolution theorem, giving a new form of the expression for the flux.

Let us switch to a reduced distribution $v = f/f^{eq}$; once the derivative of the pre-exponential $A(R)$ in the expression for f^{eq} is neglected, one has

$$\frac{\partial v}{\partial t} + v \frac{\partial}{\partial t} \ln f^{eq} = \frac{\partial}{\partial R} \beta \frac{\partial v}{\partial R} + \dot{R} \frac{\partial v}{\partial R}. \quad (20)$$

Further, consider the reduced size $r = R/R_*$ and, with $\beta_* \equiv \beta(R_*)$, define

$$\dot{r}(r) \equiv \frac{\beta \phi'(r)}{\beta_* \phi''(1)}. \quad (21)$$

Equation (20) then can be cast in the form

$$\frac{1}{2} \epsilon^2 \frac{\partial}{\partial r} \beta \frac{\partial v}{\partial r} + \dot{r} \frac{\partial v}{\partial r} - \mathcal{N} v \psi(r) \approx \frac{\partial v}{\partial t}. \quad (22)$$

The left-hand boundary condition is time-independent: $v(0,t) = 1$. Time-dependence of the barrier is now explicitly indicated by the parameter \mathcal{N} . The leading time-dependence of the critical size is contained within the function $\psi(r)$, Eq. (16). Other terms proportional to dR_*/dt , which appear due to the change of variables, can be shown to be small in ϵ [18,20(a)] and are neglected in Eq. (22). With an appropriate modification of \dot{r} , this equation is also valid for the discrete BDE in the domain $r \lesssim 1$ with a smooth $v(r)$ [20(a)].

Further, at this stage let us temporarily ignore the weak time dependence of ϵ and \mathcal{N} , and introduce a Laplace transform

$$V(r,p) = \int_0^\infty v(r,t) e^{-pt} dt.$$

Since $v(r,0) = 0$ one has

$$\epsilon^2 \frac{d}{dr} \beta \frac{dV}{dr} + 2\dot{r} \frac{dV}{dr} - 2(p + \mathcal{N}\psi)V = 0 \quad (23)$$

with the boundary condition on the left

$$V(0,p) = 1/p. \quad (24)$$

Conversion from a partial differential to an ordinary differential equation simplifies the singular perturbation analysis.

Equation (23) contains a boundary layer near $r=1$, thus two outer and one inner solution should be considered. First, consider the left-hand outer solution at $0 \leq r < 1$. Neglecting the ϵ -term, and introducing a positive “decay time”

$$t_d(r) = \int_0^r \frac{dr'}{-\dot{r}} \quad (25)$$

one has

$$V(r,p) = \frac{1}{p} \exp \left[-pt_d(r) + \mathcal{N} \int_0^r \frac{dr'}{\dot{r}'} \psi \right]. \quad (26)$$

At this point, inversion of the Laplace transform would give

$$v(r,t) = \Theta[t - t_d(r)] \exp \left(\mathcal{N} \int_0^r \frac{dr'}{\dot{r}'} \psi \right),$$

which generalizes the corresponding expression for the pure transient problem with $\mathcal{N}=0$ [20(a)]. However, matching of asymptotes is more conveniently executed in terms of the Laplace transform, and we postpone its inversion until the inner region is traversed.

In order to describe the inner solution at $|r-1| \ll 1$, we switch to the stretched variable $z=(r-1)/\epsilon$ and linearize coefficients near $r=1$. One has

$$\frac{d^2 V}{dz^2} + 2z \frac{dV}{dz} - 2mV = 0, \quad m = p + \mathcal{N}. \quad (27)$$

This is the standard equation for the repeated error integrals $i^m \operatorname{erfc}(\pm z)$ as defined by Abramowitz and Stegun [27]. Leaving only the plus sign (the “-” has a wrong asymptote at $z \rightarrow +\infty$) one thus has

$$V(z,p) = \frac{1}{2} A_m i^m \operatorname{erfc}(z). \quad (28)$$

The asymptote of $i^m \operatorname{erfc}(z) \sim 2(-z)^m / \Gamma(m+1)$ as $z \rightarrow -\infty$ should be matched with the asymptote of Eq. (26) as $r \rightarrow 1^-$, which is given by

$$V(r,p) \sim (1-r)^m \exp(\mathcal{N}C + pC'), \quad C = \int_0^1 dr \left(\frac{\psi}{\dot{r}} - \frac{1}{r-1} \right) \quad (29)$$

with C' defined in Eq. (19). This allows one to obtain the constant A_m in the inner solution:

$$A_m = p^{-1} \Gamma(m+1) e^{\mathcal{N}C + pC'} \epsilon^m. \quad (30)$$

For the asymptote into the growth region $z \rightarrow +\infty$ with $i^m \operatorname{erfc}(z) \sim (2/\sqrt{\pi}) e^{-z^2} / (2z)^{m+1}$ one thus obtains,

$$V(z,p) \sim \frac{1}{p} \epsilon^m e^{\mathcal{N}(C-C') + mC'} \Gamma(m+1) \frac{1}{\sqrt{\pi}} \frac{e^{-z^2}}{(2z)^{m+1}}. \quad (31)$$

Due to the presence of a rapidly decaying factor e^{-z^2} , matching with the growth region in terms of the reduced distribu-

tion V is inconvenient, and one should switch to a smooth nonreduced distribution V^{feq} , or directly to the flux. (Such a transition is especially important for the discrete, Becker-Döring form of the nucleation equation [20(a),28], but makes direct sense in the continuous case as well since f^{feq} has no physical meaning at $R > R_*$, and the ratio f/f^{feq} is not a “good” variable here). In the inner region the flux is given by

$$j(z,t) = -j_s \sqrt{\pi} e^{z^2} \frac{\partial}{\partial z} v(z,t).$$

Within the assumption of near-constant \mathcal{N} , the value of QSS flux j_s approximately changes with time as $e^{\mathcal{N}t}$. In terms of the Laplace transform this translates to

$$J(z,p) = -j_s(0) \sqrt{\pi} e^{z^2} \frac{d}{dz} V(z,p - \mathcal{N}). \quad (32)$$

This gives for $z \gg 1$

$$J(z,p) \approx j_s(0) e^{\mathcal{N}(C-C')} \frac{1}{p - \mathcal{N}} \Gamma(p+1) e^{-pt_i(z)}. \quad (33)$$

Here $t_i(z)$ is the leading asymptote of the incubation time [Eq. (19)], with $r \approx 1 + \epsilon z$. Since in current variables growth is practically time independent, the above expression can be used for larger r as well, with $t_i(z)$ replaced by $t_i(r)$. In this sense, matching with the growth region is completed.

At this point, prior to the inversion of the Laplace transform, one can already estimate the total number of nuclei formed by the end of nucleation with an increasing barrier, $\mathcal{N} < 0$:

$$\rho_\infty = \int_0^\infty dt j(r,t) \approx J(r,0) = j_s(0) e^{\mathcal{N}(C-C')} \frac{1}{-\mathcal{N}}. \quad (34)$$

The above expression is r -independent, and provides an exponential correction to the QSS approximation with $\rho_\infty^{QSS} \approx -j_s(0)/\mathcal{N}$. In practice, however, the current assumption $\mathcal{N} = \text{const}$ can be too strong, and a more accurate expression will be suggested.

B. Inversion of the Laplace transform

Consider first $\mathcal{N}=0$ with $J_0(r,p) = \Gamma(p) \exp[-pt_i(r)]$. In the finite part of the complex p -plane singularities of the Γ -function are simple poles located at integer $p=0, -1, -2, \dots$ with residues $1/(-p)!$. Summation over those gives the asymptotic correspondence [20(a)] for $t_i \rightarrow \infty$

$$\Gamma(p) e^{-pt_i} \leftrightarrow \exp(-e^{-t_r}) \quad (35)$$

with t_r defined in eq. (18) and assumed *finite*.

For $\mathcal{N} \neq 0$ one has

$$J(r,p) = \frac{p}{p - \mathcal{N}} J_0(r,p) \quad (36)$$

and the convolution theorem can be used. This gives

$$\frac{1}{p-\mathcal{N}}\Gamma(p+1)e^{-pt_i} \leftrightarrow \exp(-e^{-t_r}) + \mathcal{N} \int_0^{t_r+t_i} dt' \exp(\mathcal{N}t') \exp(-e^{t'-t_r}).$$

Since t_r is finite, while t_i is large, the integration can be extended to infinity. Integrating by parts, and invoking the near-exponential behavior of $j_s(t)$, one obtains

$$j(r,t) = \int_0^\infty dt' j_s(t' + C - C') \exp[t' - t_r - \exp(t' - t_r)]. \quad (37)$$

Above is the first main result of this work; since it does not contain \mathcal{N} explicitly, reasonable accuracy is expected even for $\mathcal{N} \neq \text{const}$. For slowly changing barrier the variable part of the integrand is mostly determined by the exponential term. For $t_r > 0$ the latter has a maximum at $t' = t_r$, which determines the argument of j_s . Otherwise, in this limit the expression resembles the one for transient nucleation,

$$j(r,t) \approx j_s(t_r + C - C') \exp(-e^{-t_r}), \quad |\mathcal{N}| \ll 1.$$

For $t_r < 0$, the maximum of the integrand in Eq. (37) is achieved at $t' \approx 0$, which should replace t_r in the argument of j_s in the above approximation. However, since $-t_r \lesssim 1$ [to ensure nonzero $\exp(-e^{-t_r})$], for a slowly changing j_s the approximation can be used for negative t_r as well.

In case \mathcal{N} is not necessarily small but is near-constant, the integral in Eq. (37) is evaluated in terms of an incomplete gamma-function $\Gamma(a,x)$, as defined by Abramowitz and Stegun [27]. One has

$$j(r,t) \approx j_s(t_r) \Gamma[\mathcal{N} + 1, \exp(-t_r)] \exp[\mathcal{N} \cdot (C - C')]. \quad (38)$$

This generalizes a similar expression in Ref. [19] for arbitrary ψ in Eq. (29) or, equivalently, for arbitrary $d \ln R_*/d \ln B$. In practice, when \mathcal{N} slowly drifts with time, it should be evaluated at $t = t_r$. With this, Eq. (38) is entirely determined by parameters evaluated at the retarded time t_r ; in “physical” variables the flux is sensitive to the current instant of time as well—this will become apparent once the original units are restored for comparison with numerics.

The difference $C - C'$ indicates sensitivity to a nucleation model and to the type of external control. For continuous models one can express this difference in terms of diffusivity β

$$C - C' = \varphi''(1) \left(\int_0^1 dr \frac{\beta_* \varphi - 1}{\beta \varphi'} - \nu \int_0^1 dr \frac{\beta_*}{\beta} r \right). \quad (39)$$

With $\beta \propto r^{-2-\theta}$ and ϕ defined in Eq. (3) one thus has

$$C - C' = \frac{1}{\theta + 2} + \frac{1}{\theta + 3} + \frac{2(3\nu - 1)}{\theta + 4}. \quad (40)$$

Individual values of the two constants in a general case are nonelementary, and are expressed in terms of a digamma function or, for integer θ in terms of harmonic numbers.

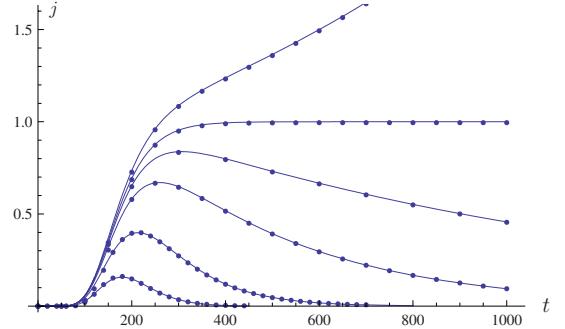


FIG. 1. (Color online) Time dependence of the reduced nucleation flux $j(R,t)/j_s(0)$ at $R \approx 1.3R_*$ for different values of \mathcal{N} at $t = 0$. From top to bottom: $\mathcal{N} = +0.05, 0.00, -0.05, -0.15, -0.5, -1.5$. Lines—Eq. (38), symbols—numerical solutions of the Zeldovich-Frenkel equation.

Qualitative structure of the flux for $\nu = 0$ is shown for different \mathcal{N} in Fig. 1; note that “physical” units are used in this and subsequent figures, and that \mathcal{N} slightly drifts with time. For $\mathcal{N} < 0$, the increasing barrier, the curves pass through a maximum at $t = t^*$. For small values of $-\mathcal{N}$ this maximum is achieved at large times $t \gg t_i(r)$, and has a value close to $j_s(0)$. For large $-\mathcal{N}$ the maximum is located close to $t_i(r)$, and is exponentially suppressed. More accurately, the retarded time corresponding to the maximum is given by

$$t_r^* \sim \begin{cases} -\ln(-\mathcal{N}), & \mathcal{N} \rightarrow 0^- \\ 1/(-\mathcal{N}e), & \mathcal{N} \rightarrow -\infty \end{cases}. \quad (41)$$

The QSS limit is recovered for both signs of \mathcal{N} in the limit $\mathcal{N} \rightarrow 0$ if time is also scaled with $|\mathcal{N}|$ —see Fig. 2. Otherwise, deviation can be significant even for modest values of \mathcal{N} . For $\mathcal{N} < 0$ there is an overshoot of the flux over its QSS value, also observed in numerical studies [10]. This effect is especially dramatic for $\mathcal{N} < -1$, when the QSS flux decays rapidly, as $\exp(\mathcal{N}t)$, while the actual flux cannot decay faster than e^{-t} , implying persistence of transient effects. For $\mathcal{N} > -1$ transient effects eventually disappear, and the flux starts

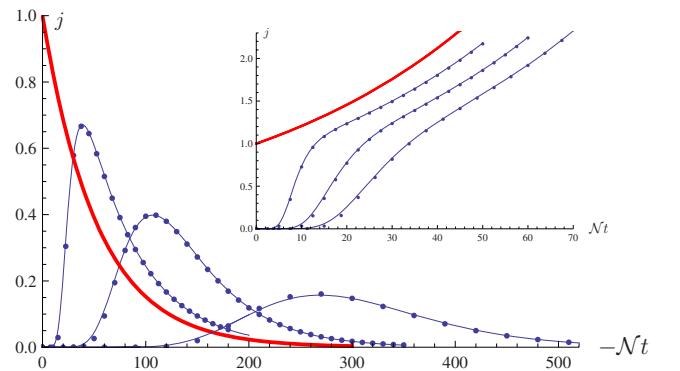


FIG. 2. (Color online) Deviation of reduced nucleation fluxes $j(R,t)/j_s(0)$ as functions of scaled times $|\mathcal{N}|t$ from the QSS curves shown by thick solid lines for $\mathcal{N} < 0$ (main panel) and $\mathcal{N} > 0$ (inset). Symbols—numerics, lines—from Eq. (38), as in Fig. 1. All \mathcal{N} are evaluated at $t = 0$. From left to right: $\mathcal{N} = -0.15, -0.05, -1.5$, and (inset) $\mathcal{N} = 0.05, 0.1, 0.15$.

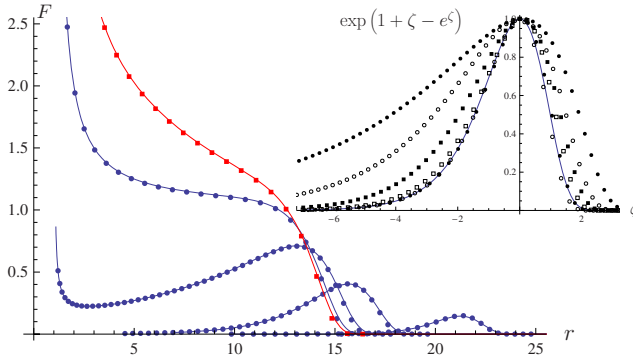


FIG. 3. (Color online) Reduced distributions $F(r, t) = f(r, t) / \tau_0 j_s(0)$ at time $t / \tau_0 \approx 26$ for different values of nonstationary index \mathcal{N} . Symbols—numerics, lines—from Eqs. (38) and (42). \mathcal{N} is evaluated at $t=0$. Descending curves: $\mathcal{N}=+0.05$ (square symbols), and $\mathcal{N}=0$; bell-shaped (from left to right) $\mathcal{N}=-0.15, -0.5, -1.5$. Inset: approaching asymptotic shape (line) as $t \rightarrow \infty$, for large negative \mathcal{N} ; $\zeta = r - r^{\max}$. Symbols—numerics at $t / \tau_0 \approx 260$. In order of diminishing width, $\mathcal{N}=-0.5, -1, -2, -4, -8$ (for the two latter sets of symbols, solid and open circles, respectively, the width is practically identical and it does not change with further increase of $|\mathcal{N}|$).

tracking the QSS limit at $t \geq t_r$, but with a significant persistent deviation corresponding to “intermediate adiabatic regime” described in Refs. [18,20(b)] for a somewhat different situation with $\nu=1/2$.

C. Distribution function

As long as variables in which growth is almost time independent are used, distribution is related to flux from Eq. (38) by

$$f(r, t) \approx j(r, t) / \dot{r}. \quad (42)$$

Typical examples are shown in the main panel of Fig. 3. In contrast to the related QSS approximation, Eq. (12) with $\theta=0$, the distributions have a smooth cutoff at large sizes and show a near-singular behavior near the critical size.

Consider several limiting cases. For small \mathcal{N} one has

$$f(r, t) \approx \frac{1}{\dot{r}} j_s(t_r) \exp[-\exp(-t_r)], \quad |\mathcal{N}| \ll 1, \quad (43)$$

where the small constant $C - C'$, which is $1/3$ in the example considered, has been dropped from the argument of j_s . Although not shown in Fig. 3, this approximation provides virtually indistinguishable results for $|\mathcal{N}| \leq 0.15$. In the formal limit $\mathcal{N} \rightarrow 0$ the cutoff described by the double-exponential factor becomes infinitely sharp on the scale of a typical size $1/|\mathcal{N}|$, the location of singularity approaches zero on that scale and the distribution acquires a QSS structure, similar to the one in Eq. (12) with $\theta=0$.

Conversely, for large negative \mathcal{N} one can use the asymptote

$$\Gamma(n+1, z) \sim \frac{z^{n+1}}{-n} e^{-z}, \quad n \rightarrow -\infty$$

to obtain

$$f(r, t) \approx \frac{1}{\dot{r}} j_s(0) \frac{\exp[\mathcal{N}(C - C')]}{-\mathcal{N}} \exp[-t_r - \exp(-t_r)], \quad -\mathcal{N} \gg 1. \quad (44)$$

The shape of the distribution is \mathcal{N} -independent, but changes with time due to interplay of $1/\dot{r}$ and the t_r -dependent part.

At large times particles grow to large sizes, and \dot{r} approaches a constant value \dot{r}_∞ (only interface-limited growth will be discussed at this point). In appropriate variables the distribution will also approach its asymptotic form. Let us introduce, as in Ref. [22] a time-dependent “front” of the distribution $r^f(t)$, which corresponds to $t_r=0$ and is given by the root of the equation

$$t = t_r(r^f). \quad (45)$$

With the scaled distance from that front

$$\zeta = \frac{r - r^f(t)}{\dot{r}_\infty} \quad (46)$$

one can cast the asymptotic distribution $f(\zeta) = f(r, t) \dot{r}_\infty$ as

$$f(\zeta) \approx j_s(0) \exp[\mathcal{N}(C - C')] e^{-\mathcal{N}\zeta} \Gamma(\mathcal{N} + 1, e^\zeta). \quad (47)$$

For $\mathcal{N} \geq 0$ this distribution decays monotonically with ζ . For $\mathcal{N} < 0$ there will be a maximum at $\zeta < 0$. For $|\mathcal{N}| \ll 1$ the variable part of $f(\zeta)$ is given by

$$f \propto \exp(-\mathcal{N}\zeta - e^\zeta),$$

with a maximum at $\zeta \approx \ln(-\mathcal{N})$ and a strong asymmetry with a long tail $\sim 1/(-\mathcal{N})$ at $\zeta < 0$ and a sharp cutoff at positive $\zeta \sim 1$.

For large $-\mathcal{N}$ one has

$$f(\zeta) \approx \frac{j_s(0)}{-\mathcal{N}} \exp[\mathcal{N}(C - C')] \exp(\zeta - e^\zeta). \quad (48)$$

Remarkably, the shape of the distribution given by the ζ -dependent part of the above expression, is identical to the one which emerges in a very different situation, in case of a short nucleation pulse [22]. Another unexpected feature of this distribution is that its width becomes independent of \mathcal{N} , as illustrated in the inset of Fig. 3 where numerical data were reduced by corresponding maximal values.

One should note, however, that analytical extension of the results toward arbitrary large r was possible due to a constant value of the critical size, with a growth rate which has no explicit time dependence and thus allows a separation of variables. Otherwise, with $R_* = R_*(t)$, one should write in the Zeldovich-Frenkel model

$$\frac{dr}{dt} = 1 - \frac{1}{r} + \lambda r, \quad \lambda \equiv -d \ln R_*/dt. \quad (49)$$

Here λ has a small value of the order of $\nu\mathcal{N}/B$, so that it could be neglected when solving the nucleation part of the problem and when evaluating $f(r, t)$ up to moderate sizes r . Eventually particles will grow to sizes $r \geq 1/|\lambda|$, when the corresponding term in Eq. (49) becomes important. Here, however, the nonreduced growth rate $dR/dt \approx R_*$ is size independent, implying that the shape of the distribution $f(R, t)$

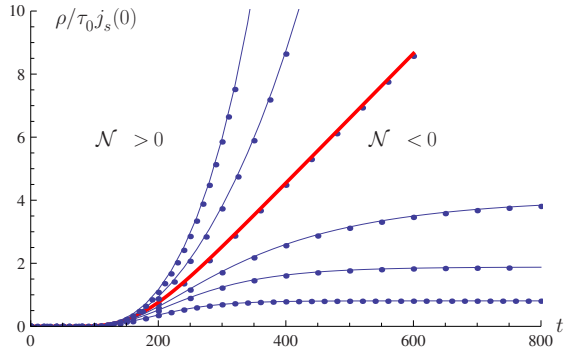


FIG. 4. (Color online) Reduced number of particles with size exceeding a selected value of $R \approx 1.3R_*$ for different values of non-stationary index \mathcal{N} . Symbols—numerics, lines—Eq. (53). Clockwise: $\mathcal{N}(0)=0.5, 0.25, 0, -0.25, -0.5, -1$. The pure transient curve for $\mathcal{N}=0$ [thick solid line, Eq. (52)], which becomes linear at large t , separates the regions of exponential growth at $\mathcal{N}>0$ and of saturation at $\mathcal{N}<0$, when the $\rho(t)$ curves tend to R -independent constants shown in Fig. 5.

will not change anymore, and allowing one to utilize the above results. In practice, difficulties of this kind can be avoided if one does not attempt to construct an analytical expression for the distribution at all sizes (which inevitably involves additional approximations for growth if $R_* \neq \text{const}$), but rather treats the flux $j(r_0, t)$ at some reasonably small $r_0 > 1$ as the “nucleation rate.” The nucleated particles can then be grown numerically with an accurate growth rate corresponding to a variable R_* , and insensitivity of the resulting distribution to selection of r_0 will indicate the consistency of such a combined approach.

D. Number of nuclei

The number of nuclei with size exceeding a given value r is given by

$$\rho(r, t) = \int_0^t dt' j(r, t'). \quad (50)$$

Consider first the case $\mathcal{N}=\text{const}$ when the flux is expressed through the incomplete gamma function, Eq. (38), and the integral can be evaluated explicitly. Using the identity

$$\int_Z^\infty z^{-n-1} \Gamma(n+1, z) dz = Z^{-n} \Gamma(n, Z) = E_{1-n}(Z),$$

where $E_m(z)$ is the standard exponential integral [27], one obtains

$$\rho(r, t) \approx j_s(0) \exp[\mathcal{N}(C - C')] E_{1-\mathcal{N}}(e^{-tr}). \quad (51)$$

In the limit of pure transient nucleation $\mathcal{N}=0$ the above expression is reduced to [20(b)]

$$\rho_0(r, t) = j_s E_1(e^{-tr}), \quad (52)$$

which is shown by a thick solid line in Fig. 4 together with numerical data.

For $\mathcal{N} \neq \text{const}$ it is better to start with the integral representation of the flux, Eq. (37), and switch to integration with

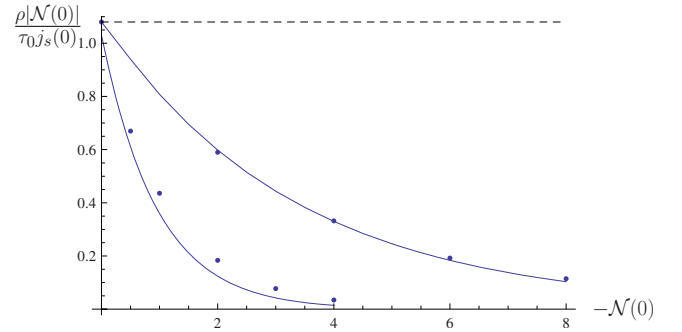


FIG. 5. (Color online) Scaled total number of nuclei as a function of dimensionless rate of the barrier increase $\tau_0 dB/dt = -\mathcal{N}(0)$ for two alternative time dependences of the critical size. Symbols—numerics, solid lines—Eq. (54) with $C-C'=1/3$ (upper, $R_*= \text{const}$) and $C-C'=13/12$ [lower, $R_* \propto \sqrt{B(t)}$]—see text. Horizontal dashed line is the QSS approximation, Eq. (55).

respect to t_r , with the lower limit extended to $-\infty$ when evaluating ρ . Since only the exponential term depends on t_r , one obtains

$$\rho(r, t) = \int_0^\infty dt' j_s(t' + C - C') \exp[-\exp(t' - t_r)]. \quad (53)$$

Typical time dependences of the number of nuclei are shown in Fig. 4. Results are accurate at least for the numerical examples considered with $R_*= \text{const}$ (i.e., $C-C'=1/3$). Equation (51) (not shown in the figure) could provide an almost comparable accuracy, but in each case this equation requires a selection of a single representative \mathcal{N} which is not constant throughout the process. From an experimental point, observation of the entire $\rho(t)$ curve usually requires some non-trivial technique, such as two-step annealing [12] in isothermal crystal nucleation studies, which would correspond to $\mathcal{N}=0$ (thick solid line) in Fig. 4. Otherwise, of potential experimental relevance is the *final* value ρ_∞ , which is defined only for $\mathcal{N}<0$, and which is independent of the size r .

With the identity

$$E_{1-n}(0) = -1/n, \quad n < 0$$

at $t \rightarrow \infty$ Eq. (51) is reduced to Eq. (34). As mentioned, however, that expression is sensitive to selection of \mathcal{N} for $\mathcal{N} \neq \text{const}$, and in a general case better accuracy is achieved by the large time limit of Eq. (53),

$$\rho_\infty \approx \int_0^\infty dt j_s(t + C - C'). \quad (54)$$

The QSS limit

$$\rho_\infty^{QSS} = \int_0^\infty j_s(t) dt \approx j_s(0) / [-\mathcal{N}(0)] \quad (55)$$

is recovered for slow barrier change, when the constant $C - C'$ in Eq. (54) is negligible on a characteristic time scale $-1/\mathcal{N}$. Typical non-QSS corrections are shown in Fig. 5 where, unlike previous figures with $C-C'=1/3$ (fixed critical size) the experimentally more realistic case of $C-C'=13/12$ (i.e., $d \ln R_*/d \ln B = 1/2$) also is included. In both

cases analytical predictions reproduce the reduction of the number of nuclei compared to QSS approximation; a certain loss of numerical accuracy for $R_* \neq \text{const}$ is due to neglect of related small corrections in Eq. (22).

IV. MODEL AND COMPARISON WITH NUMERICS

At this point, the original “physical” time t will be restored. This implies that all t 's in the previous section should be understood as \tilde{t} and all fluxes j as \tilde{j} [thus, for example if one needs to deduce the physical flux $j(r, t)$ from Eq. (38), the latter should be divided by $\tau(t)$].

The Zeldovich-Frenkel model corresponds to interface-limited growth with $\theta=0$, i.e.,

$$\dot{R} = \frac{R_*}{\tau} \left(1 - \frac{1}{r} \right) \quad (56)$$

and $\beta \propto R^{-2}$ in Eq. (1). Equation (19) for the incubation time is then reduced to [20(b)]

$$\tilde{t}_i(r) = r - 2 + \ln[6B(r-1)]. \quad (57)$$

This allows one to evaluate the dimensionless retardation time $\tilde{t}_r = \tilde{t} - \tilde{t}_i(r)$ and, after evaluating the constants $C - C'$ (see below) specifies the main analytical results for the flux, distribution and the number of nuclei.

In numerical description the Turnbull-Fisher version of the general Becker-Döring equation was considered, with the gain coefficient $\beta_n = n^{2/3} \exp[(W_n - W_{n+1})/2kT]$,

$$\frac{df_n}{dt} = j_n - j_{n+1}, \quad j_n = \beta_{n-1} f_{n-1} - \alpha_n f_n. \quad (58)$$

The loss $\alpha_n = \beta_{n-1} \exp[(W_n - W_{n-1})/kT]$ follows from detailed balance. Except for the time scale, the model is standard in nucleation description [6,10,16,17], but the critical size was selected at a large number, $n_* \geq 6^3 = 216$, so that accurate correspondence with the Zeldovich-Frenkel model is expected due to small values of the “discreteness parameter” $a = 2B/n_*$. The number of Becker-Döring equations was taken as $n^{\text{max}} = 400$, with boundary conditions $f_n = 1$ at $n = 1$ and $f_n = 0$ at $n = n_{\text{max}} + 1$. The flux j_n at $n = n^{\text{up}} = 380$ was treated as “nucleation rate;” once nucleated, particles were grown deterministically in accord with Eq. (56). Conversion between the n - and the r -spaces was done in accord with $f(r, t) = f_n(t) 3n_* r^2$, and $r = (n/n_*)^{1/3}$. Consistency was tested by the overlap of the Becker-Döring and the deterministic distributions between n^{up} and n^{max} . The realization of numerics was similar to the one described in Ref. [22(b)], but with update replaced by the more stable Crank-Nicolson scheme. The actual run required two dimensionless time-dependent input parameters, $B(t)$ and $n_*(t)$.

With the above selection of β_n , the main time scale is given by

$$\tau = \frac{3 n_*^{4/3}}{2 B}. \quad (59)$$

Time dependence for most examples was taken as

$$B(t) = B_0(1 - bt), \quad n_* = \text{const}. \quad (60)$$

This gives $\mathcal{N} = B_0 b \tau$, $C - C' = 1/3$, and

$$t(\tilde{t}) = \frac{1}{a} (1 - \sqrt{1 - 2b\tau_0 \tilde{t}}) \quad (61)$$

with $\tau_0 \equiv \tau(0)$. On a single occasion, when evaluating ρ_∞ (the last figure) the critical size also was taken as time-dependent

$$n_*(t) = n_*^0 (1 - bt)^{3/2}.$$

This leads to $\nu \equiv d \ln R_*/d \ln B = 1/2$ and to $C - C' = 13/12$; the expression for $t(\tilde{t})$ is somewhat more cumbersome in that case, but is quite straightforward and is left to the reader. The initial critical size had the same value $n_*^0 = 216$, and the same typical initial barrier $B_0 = 40$ was used.

V. DISCUSSION

In the general nucleation problem described within the context of Becker-Döring equation (BDE), there are two semi-independent large parameters—the dimensionless barrier B and the critical cluster number n_* . In steady-state the situation is dominated by the barrier, which determines the exponential part of the flux j_s , while the critical size has only minor effect on the pre-exponential. A similar situation is encountered for slowly changing parameters within the adiabatic or quasi-steady-state (QSS) approximation. However, by ignoring the \dot{B} and the \dot{n}_* dependences, the QSS approximation predicts incorrect scaling, as in Figs. 2 and 5. On the other hand, accuracy of the time-dependent treatment can be restored based on the matched asymptotic approach to BDE, revealing the sensitivity of non-QSS corrections to both \dot{B} and \dot{n}_* .

The simplest, yet nontrivial situation arises for a time-dependent barrier but a large fixed critical size (as, for example in a cold magnetic system with variable temperature but small constant external field). In such cases the starting approximation to BDE, Eq. (22) is near-exact, while growth to arbitrary sizes also can be described accurately, removing the necessity of additional approximations when evaluating the distribution function. As a result, numerical accuracy of related asymptotic results is also high, as in Figs. 1–5. For $n_* \neq \text{const}$ the accuracy can be less impressive—see the lower curve in Fig. 5—although the results remain qualitatively correct. However, care should be taken in case of a very rapid change of n_* on a time scale τ , as in nucleation problems in the vicinity of a glass transition [11].

The main results, e.g., Eq. (37) for the flux or Eqs. (53) and (54) for the number of nuclei, are sensitive to both the barrier changes and—via the constant C —to dn_*/dt . Once the barrier change rate is near-constant, and is characterized by a dimensionless “nonstationary index” $\mathcal{N} = -\tau dB/dt$, an explicit \mathcal{N} -dependence is observed, although still in terms of nonelementary incomplete gamma function (or the equivalent exponential integral). The latter is due to a simultaneous presence of transient effects, which account for sensitivity to initial conditions (i.e., to the instant when nucleation starts), and of the retardation effects, which account for sensitivity to

past values of the barrier. Simplifications are possible for small $|\mathcal{N}|$ —see, e.g., Eq. (43) for the distribution function. For positive and moderately negative $\mathcal{N} > -1$ transient effects eventually disappear, and the system approaches an intermediate quasiadiabatic regime [18,20(a)], which is not close to QSS for finite \mathcal{N} . For a fast increase of the barrier $\mathcal{N} < -1$ transient effects persist, and the system never forgets the initial conditions. For large $-\mathcal{N}$ the distribution approaches a universal \mathcal{N} -independent shape, surprisingly similar to the one which appears in a rather different physical context [22].

In view of potential applications, one should note that current results were obtained and tested for finite, slowly changing \mathcal{N} , of a constant sign. For situations when those conditions can be violated, such as the aforementioned vicinity of the glass transition or the nonmonotonic change of the barrier, further analysis is required. Also, as discussed in Sec.

III C, at very large sizes the obtained distributions can be affected by a variable $n_*(t)$, even if the latter changes slowly. This can be especially important for an increasing barrier with $\mathcal{N} < 0$, when nucleation eventually stops and growth remains the only reason for the distribution to change. Furthermore, when particles grow to exponentially large sizes with a nonvanishing value of $n\rho$ (if the nucleation rate and the number of particles ρ are normalized per monomer) they start depleting the metastable phase. This increases the barrier and the critical size, as in the Lifshits-Slyozov-Wagner (LSW) scenario [29], and strictly speaking, is beyond the current study which assumes that dependences $B(t)$ and $n_*(t)$ are known *a priori*. Nevertheless, most likely small depletion effects can be included iteratively, and otherwise the obtained distributions can serve as initial conditions for subsequent independent description of growth and transition to later stages of LSW-type.

-
- [1] Ya. B. Zeldovich, *Acta Physicochim. URSS* **18**, 1 (1943).
- [2] F. F. Abraham, *Homogeneous Nucleation Theory* (Academic Press, New York, 1974).
- [3] J. Wölk, R. Strey, C. H. Heath, and B. E. Wyslouzil, *J. Chem. Phys.* **117**, 4954 (2002).
- [4] R. S. Sidin, R. Hagmeijer, and U. Sachs, *Phys. Fluids* **21**, 073303 (2009); V. Holten and M. E. H. van Dongen, *J. Chem. Phys.* **130**, 014102 (2009); D. van Putten and V. Kalikmanov, *ibid.* **130**, 164508 (2009).
- [5] K. F. Kelton and A. L. Greer, *Nucleation in Condensed Matter: Applications in Materials and Biology* (Elsevier, New York, 2010).
- [6] K. F. Kelton and A. L. Greer, *J. Non-Cryst. Solids* **79**, 295 (1986).
- [7] V. A. Shneidman, *Phys. Rev. Lett.* **75**, 4634 (1995); *J. Chem. Phys.* **103**, 9772 (1995).
- [8] S. R. Stiffler, M. O. Thompson, and P. S. Peercy, *Phys. Rev. B* **43**, 9851 (1991).
- [9] V. A. Shneidman, *J. Appl. Phys.* **80**, 803 (1996).
- [10] K. F. Kelton, *J. Non-Cryst. Solids* **163**, 283 (1993).
- [11] V. A. Shneidman, *J. Chem. Phys.* **102**, 1791 (1995); V. A. Shneidman and M. C. Weinberg, *J. Non-Cryst. Solids* **194**, 145 (1996).
- [12] P. P. James, *Phys. Chem. Glasses* **15**, 95 (1974); J. Deubener, R. Brückner, and M. Sternizke, *J. Non-Cryst. Solids* **163**, 1 (1993).
- [13] V. A. Shneidman and D. R. Uhlmann, *J. Chem. Phys.* **109**, 186 (1998).
- [14] Y. Farjoun and J. C. Neu, *Phys. Rev. E* **78**, 051402 (2008).
- [15] F. M. Kuni, A. K. Shchekin, and A. P. Grinin, *Phys. Usp.* **44**, 331 (2001).
- [16] K. F. Kelton, A. L. Greer, and C. V. Thompson, *J. Chem. Phys.* **79**, 6261 (1983).
- [17] L. Gránásy and P. James, *J. Chem. Phys.* **113**, 9810 (2000).
- [18] V. A. Shneidman, *Sov. Phys. JETP* **64**, 306 (1986).
- [19] V. A. Shneidman and P. Hänggi, *Phys. Rev. E* **49**, 641 (1994).
- [20] V. A. Shneidman, *Sov. Phys. Tech. Phys.* **32**, 76 (1987); **33**, 1338 (1988); *J. Chem. Phys.* **127**, 041102 (2007).
- [21] V. A. Shneidman and I. M. Fishman, *Chem. Phys. Lett.* **173**, 331 (1990).
- [22] V. A. Shneidman, *Phys. Rev. Lett.* **101**, 205702 (2008); *J. Chem. Phys.* **131**, 164115 (2009).
- [23] E. M. Lifshits and L. P. Pitaevskii, *Physical Kinetics* (Pergamon Press, New York, 1981).
- [24] V. A. Shneidman, *Phys. Rev. Lett.* **95**, 115701 (2005).
- [25] V. A. Shneidman and M. C. Weinberg, *J. Chem. Phys.* **97**, 3621 (1992); **97**, 3629 (1992).
- [26] V. A. Shneidman and R. K. P. Zia, *Phys. Rev. B* **63**, 085410 (2001).
- [27] M. Abramowitz and I. Stegun, *Handbook of Mathematical Functions* (Dover, New York, 1972).
- [28] V. A. Shneidman, *Phys. Lett. A* **143**, 275 (1990).
- [29] I. M. Lifshits and V. V. Slyozov, *Zh. Eksp. Teor. Fiz.* **35**, 479 (1958); C. Wagner, *Z. Elektrochem.* **65**, 581 (1961).